Fluorescence Anisotropy of Hydrophobic Probes in Poly(*N*-decylacrylamide)-*block*-poly(*N*,*N*-diethylacrylamide) Block Copolymer Aqueous Solutions: Evidence of Premicellar Aggregates

Mariana Beija,[†,‡,§] Aleksander Fedorov,[†] Marie-Thérèse Charreyre,[‡,∥] and José M. G. Martinho*[,†]

Centro de Química-Física Molecular and IN - Institute of Nanoscience and Nanotechnology, Instituto Superior Técnico, Av. Rovisco Pais 1, 1049-001 Lisbon, Portugal, and Unité Mixte CNRS-bioMérieux, École Normale Supérieure de Lyon, 46 Allée d'Italie, 69364 Lyon Cedex 07, France

Received: February 23, 2010; Revised Manuscript Received: June 11, 2010

Fluorescent probes, coumarin 153 (C153) and octadecylrhodamine B (ORB), were used to study the self-assembly in water of poly(*N*-decylacrylamide)-*block*-poly(*N*,*N*-diethylacrylamide), ($PDcA_{11}$-*block*-$PDEA_{295}$; $M_n = 40\ 300$ g mol^{-1}; $M_w/M_n = 1.01$). From the variation of both the fluorescence intensity and the solvatochromic shifts of C153 with polymer concentration, the critical micelle concentration (CMC) was determined as 1.8 ± 0.1 μM. On the other hand, steady-state anisotropy measurements showed the presence of premicellar aggregates below the CMC. Time-resolved fluorescence anisotropy evidenced that ORB is located in the premicellar aggregates and the micelle core, while C153 is partitioned between the aggregates and the water phase. The micelle core contains both semicrystalline and amorphous regions. In the semicrystalline regions the probes cannot rotate, while in the amorphous regions the rotational correlation times correlate well with the hydrodynamic volume of the probes. The amorphous region of the micelle core is relatively fluid, reflecting the large free-volume accessible to the probes.

Introduction

The self-assembly of amphiphilic molecules in aqueous solutions has many technological applications, which motivated several studies in the last years.[1] For nonionic surfactants, the micellization process is driven by the balance between minimization of oil−water interface energy and maximization of entropy—the so-called *hydrophobic effect*. In the case of ionic surfactants, the electrostatic repulsion of equally charged heads has also to be considered.[2] Although it is generally accepted that the major processes of self-assembling of molecular and macromolecular amphiphiles start to occur at a well-defined concentration, the critical micelle concentration (CMC), several experimental[3−6] and theoretical[7−9] studies point toward the formation of aggregates at concentrations well below the CMC—a phenomenon known as *premicellar aggregation*—even for low molecular weight surfactants. The presence of premicellar aggregates was for instance demonstrated by fluorescence correlation spectroscopy (FCS) of aqueous solutions of low molecular weight surfactants. The fluorescence correlation functions of several fluorescent probes (cresyl violet, sulforhodamine B, and sulforhodamine G) showed the coexistence of two populations of dye molecules, one characterized by the diffusion time of the free probe and another characterized by a considerably larger diffusion time (at concentrations between about 0.3 × CMC and the CMC), indicating the presence of premicellar aggregates.[4] These results are supported by the theoretical work of Hadgiivanova and Diamant[7] based on a two-state (unimer-aggregate) model that predicts the existence of three well separated transitions at different surfactant concentrations: *C*1, where metastable aggregates exist but not in a significant extent; *C*2, above which an appreciable amount of metastable aggregates forms; *C*3, where the aggregated state becomes stable (corresponding to the CMC). Hence, significant premicellar aggregation occurs in the concentration range between *C*2 and *C*3. Moreover, these authors demonstrated that the extent of premicellar aggregation was much larger than expected from mere finite-size effects and that the premicellar regime was characterized by a weak concentration dependence of micelle size.[7] More recently, the same authors showed that the premicellar aggregates are kinetically stable in most of the premicellar region, and that the range of stability becomes wider with the increase of the surfactant hydrophobicity. The premicellar aggregates have narrow size distributions with polydispersity slightly higher than their micelle counterparts.[8] Both experimental and theoretical results support the existence of premicellar aggregates that cannot be detected by the commonly used methods for CMC determination such as conductivity and surface tension.

Time-resolved fluorescence anisotropy has been widely used to probe the molecular dynamics of a fluorophore within a micelle. Important information about both the viscosity of the micelle core and the overall motion of the micelle can be obtained. The dynamics of various fluorescent probes were reported for low molecular weight surfactants such as SDS,[10−13] CTAB,[10−12] Triton X-100,[10,14−17] Brij-35,[18] and AOT[19] as well as for polymeric surfactants such as PEO-PPO-PEO[20,21] and Thesit.[11,12] Moreover, the interactions between peptides and

* To whom correspondence should be addressed. Fax:+351 218464455. Phone: +351 218419250. E-mail: jgmartinho@ist.utl.pt.
† Instituto Superior Técnico.
‡ École Normale Supérieure de Lyon.
§ Current address: Laboratoire des Interactions Moléculaires et Réactivité Chimique et Photochimique, UMR 5623, Université Paul Sabatier, 31062 Toulouse Cedex 9, France.
∥ Current address: Laboratoire Joliot-Curie et Laboratoire Ingénierie des Matériaux Polymères, ENS, IFR128, 46 Allée d'Italie 69364 Lyon Cedex 07, France.

10.1021/jp101613y
Published on Web 07/16/2010

micelles[11,12] and the influence of additives[13,17] and temperature[18] on the rotational relaxation of the probe have also been studied. However, these studies were performed at concentrations much higher than the CMC, where the presence of premicellar aggregates is not detected.

In this work, steady-state and time-resolved fluorescence anisotropy measurements were carried out using coumarin 153 (C153) and octadecylrhodamine B (ORB) as fluorescent probes to study the formation of premicellar aggregates of poly(*N*-decylacrylamide)-*block*-poly(*N*,*N*-diethylacrylamide) ($PDcA_{11}$-*block*-$PDEA_{295}$) (Scheme 1). C153 was chosen since it presents a very strong solvatochromism (owing to the large difference between the dipole moments of the ground and excited states[22]) that enables an easy detection of changes in its environment. Because of these properties, this dye has been extensively employed for studies of solvation dynamics[23−32] and, occasionally, for probing the local environment of starlike polymers[33] and block copolymer micelles.[34,35] On the other hand, ORB was used because, owing to the high hydrophobicity of the C18 alkyl chain, it is almost insoluble in water and presents a high tendency to be located in the micelle core.[14,36,37]

SCHEME 1: Molecular Structures of Probes, Coumarin 153 (C153) and Octadecylrhodamine B (ORB), and Amphiphilic Block Copolymer, Poly(*N*-decylacrylamide)-*block*-poly(*N*,*N*-diethylacrylamide), $PDcA_{11}$-*block*-$PDEA_{295}$ (M_n = 40 300 g mol^{-1}; M_w/M_n = 1.01) Used in This Study

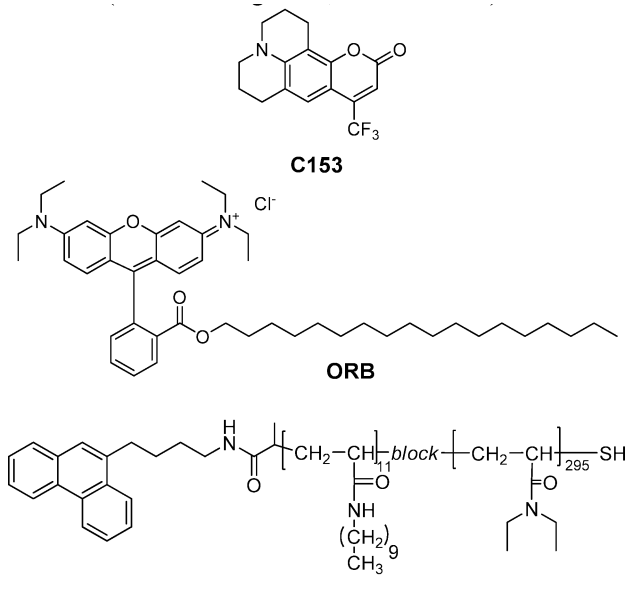

Experimental Section

Materials. The fluorescent probes coumarin 153 (C153) (≥99.9% by HPLC) and octadecylrhodamine B (ORB) (fluorescence grade) were purchased from Fluka and Molecular Probes, respectively. The purity of both probes was further verified by UV−vis absorption and fluorescence and they were used without further purification. THF (Sigma-Aldrich, 99.9%) was freshly distilled under argon to remove the inhibitor. Water was distilled twice and deionized with Millipore Milli-Q system. Ethanol (Fluka, 99.9%), hexylamine (Aldrich, 99%), and *n*-hexane (Fluka, 95%) were used as received.

The block copolymer sample, $PDcA_{11}$-*block*-$PDEA_{295}$ (M_n = 40 300 g mol^{-1}; M_w/M_n = 1.01) was previously synthesized by sequential RAFT polymerization.[38] It was further treated with a large excess of hexylamine (ca. 100 equiv) in dichloromethane at room temperature for 4 h to remove the dithiobenzoate moiety and purified by precipitation in *n*-hexane. The conversion of the dithiobenzoate moiety into a thiol group was confirmed by UV−visible absorption. The lifetime of the phenanthrene-labeled $PDcA_{11}$-*block*-$PDEA_{295}$ block copolymer bearing a thiol group at the ω-chain-end was close to the value of the phenanthrene free probe ~47 ns, proving that the thiol group is not an efficient fluorescence quencher in contrast with the dithiobenzoate moiety.[39,40]

Sample Preparation. The block copolymer solutions in water were prepared by using a solvent-assisted solubilization method, to obtain monodisperse micelles, prevent the presence of large aggregates, and uniformly solubilize the C153 in the micelle cores. THF was used because it is a good solvent for both blocks and the dye. Stock solutions of C153 (1.4×10^{-4} M) and $PDcA_{11}$-*block*-$PDEA_{295}$ (~50 g L^{-1}) were prepared in THF. Then, dilute solutions with increasing block copolymer concentrations were prepared in THF. A small volume of each polymer solution (60 μL) was transferred into small vials, immersed in an ice bath, ~2 °C, already containing the required amount of C153. Then, cold water (~2 °C) was added dropwise with gentle agitation to the required final volume. The concentrations in polymer vary from 0 to 1.1 g L^{-1} while the concentration of C153 is ~0.45 μM for all solutions. The final aqueous solutions were equilibrated (and stored) at 4 °C for at least 24 h before the fluorescence measurements (recorded at 20 °C). Previous reported experiments have demonstrated that such a THF content (always <2% v/v) does not interfere significantly with the properties of the micellar aggregates.[41,42]

Mixed solutions of ORB and block copolymer were prepared with the same experimental procedure, using a stock solution of ORB in ethanol (4.9×10^{-5} M).

Steady-State Fluorescence Measurements. Fluorescence spectra of C153 in $PDcA_{11}$-*block*-$PDEA_{295}$ aqueous solutions were acquired with a SLM-AMINCO 8100 Series 2 spectrofluorometer (bandwidths 4 nm for emission and excitation; path length 5 mm). C153 was excited at 410 nm, and the fluorescence spectra were recorded between 420 and 800 nm. For steady-state fluorescence anisotropy measurements, the sample was excited with vertically polarized light and the fluorescence polarized components, parallel ($I_{||}$) and perpendicular ($I_{\perp}$) to the direction of the excitation light, were recorded. The steady-state anisotropy (r_{ss}) was then calculated by

$$r_{ss} = \frac{I_{||} - GI_{\perp}}{I_{||} + 2GI_{\perp}} \quad (1)$$

where G is an instrumental correction factor, which takes into account the sensitivity of the monochromator to the polarization of light. The intensities $I_{||}$ and $I_{\perp}$ were acquired using Glan−Thompson polarizers and corrected for the background. The C153 samples were electronically excited by light at λ_{exc} = 420 nm and the fluorescence was recorded at λ_{em} = 530 nm, whereas for ORB the excitation wavelength was λ_{exc} = 570 nm and the fluorescence was recorded at λ_{em} = 610 nm, using in both cases a bandwidth of 16 nm for excitation and emission. The temperature was controlled with a water circulating bath from Julabo (model F25). The samples were kept, under stirring, at the desired temperature (20 ± 0.2 °C) for 30 min before measurements.

Time-Resolved Fluorescence Measurements. Time-resolved picosecond fluorescence measurements were performed by the

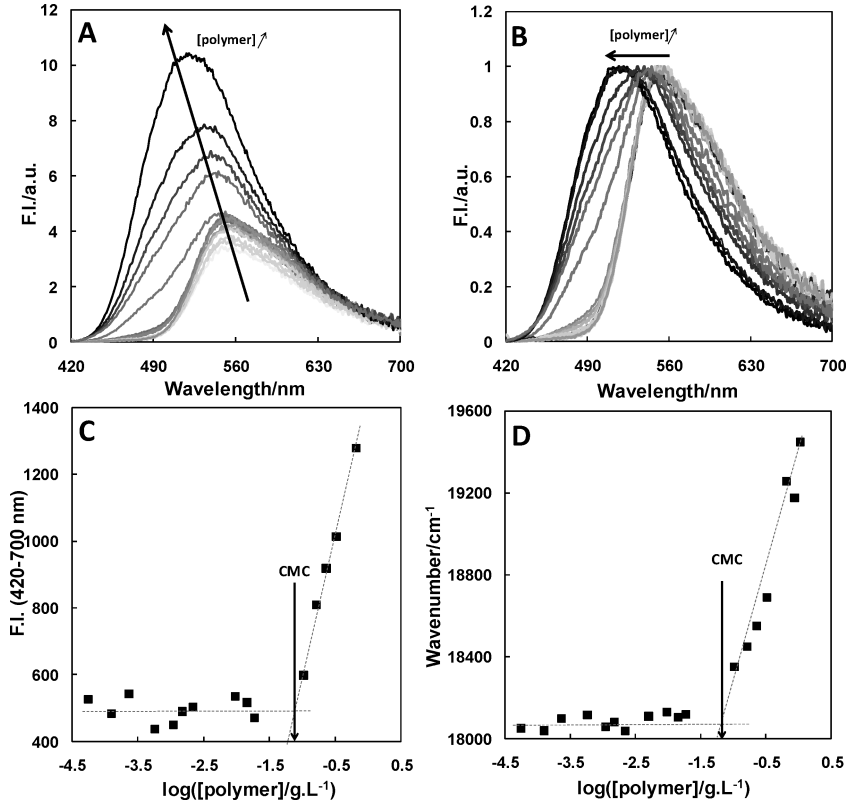

Figure 1. Fluorescence spectra (A) and normalized fluorescence spectra (B) of C153 in aqueous solutions of $PDcA_{11}$-*block*-$PDEA_{295}$ at increasing polymer concentrations. Plots of fluorescence intensity (C) and maximum emission wavenumber (D) as a function of $PDcA_{11}$-*block*-$PDEA_{295}$ concentration (g L^{-1}) (λ_{exc} = 410 nm; 20 °C; [C153] ≈ 0.45 μM).

single-photon timing (SPT) technique with two pulsed laser light sources. One system consisted of a mode-locked Spectra-Physics Vanguard 2000-HM532 Nd:YVO_4 diode laser, delivering 2 W of 533 nm light at a repetition rate of 76 MHz and pulse duration of ~12 ps that synchronously pumped a cavity dumped 710-2 dye (rhodamine 6G) laser, delivering 3−4 ps pulses at a repetition rate of 1.9 MHz. The other system consisted of a Spectra-Physics Millenia Xs Nd:YVO_4 diode laser, pumping a Spectra-Physics Tsunami titanium−sapphire laser, delivering 100 fs pulses at a repetition rate of 76 MHz. The repetition rate was decreased to 4 MHz by a pulse picker and the light frequency doubled in a LBO crystal to deliver pulses in the 360−480 nm spectral range. Intensity decay measurements were made with the emission polarizer set at the magic angle relative to the vertical polarized excitation light. Anisotropy decay measurements were made by successive collection of the instrumental response function and the vertical and horizontal polarized components, acquired during the same time interval. The fluorescence was passed through a depolarizer set at the entrance of a Jobin-Yvon HR320 monochromator with a grating of 100 lines per nm and was detected by a Hamamatsu 2809U-01 microchannel plate photomultiplier. With this setup, the *G* factor is equal to 1. The instrument response function had an effective fwhm of 35 ps.

Fluorescence intensity decay curves of C153 were obtained by pulsed excitation light at 420 nm from the titanium−sapphire laser setup and the emission collected at 530 nm, while the decays of ORB were obtained using excitation light of 570 nm from a rhodamine dye laser and the emission was recorded at 610 nm.

The decay curves were analyzed by homemade software that uses a nonlinear least-squares reconvolution method.

Results and Discussion

Determination of the CMC. The CMC of $PDcA_{11}$-*block*-$PDEA_{295}$ was determined using the variation of fluorescence intensity and spectral shifts of C153 in polymer aqueous solutions of several concentrations. Hence, copolymer aqueous solutions with concentrations ranging from ~30 μg L^{-1} to 1.1 g L^{-1} (concentration of C153 ≈ 0.45 μM) were prepared and their fluorescence spectra were recorded at 20 °C.

Figure 1 shows that both an increase in fluorescence intensity and a hypsochromic shift of the maximum emission wavelength occur as the polymer concentration increases. At a given concentration onset, a steep variation of the fluorescence intensity and a large shift in the maximum emission wavelength can be observed as a consequence of the migration of the dye from the aqueous medium to the hydrophobic micelle cores. The CMC could then be determined from the intercept of the two lines drawn for concentrations below and above the concentration at which micelles are first formed (as shown in Figure 1C,D) and it was found to be 0.072 g L^{-1} (1.8 μM) or 0.075 g L^{-1} (1.9 μM), using the fluorescence intensity or the spectral shifts, respectively.

Steady-State Fluorescence Anisotropy. To study polymer aggregation, steady-state fluorescence anisotropy measurements were carried out. Figure 2 shows the variation of steady-state fluorescence anisotropy (r_{ss}) of C153 and ORB probes with the increasing concentration of $PDcA_{11}$-*block*-$PDEA_{295}$ in aqueous solutions at 20 °C.

At low polymer concentrations, the r_{ss} values are relatively small and remain almost constant with increasing polymer concentration, which suggests that the probes rotate freely in aqueous solutions without significant interaction with the polymer chains. The r_{ss} values of ORB at these polymer

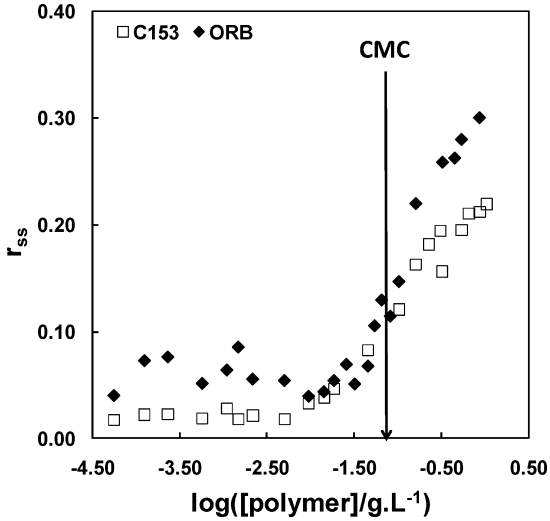

Figure 2. Steady-state fluorescence anisotropy of C153 (□) and ORB (◆) as a function of $PDcA_{11}$-*block*-$PDEA_{295}$ concentration (in g L^{-1}). [C153] ≈ 0.45 μM, λ_{exc} = 420 nm, λ_{em} = 530 nm or [ORB] ≈ 0.5 μM, λ_{exc} = 570 nm, λ_{em} = 610 nm; T = 20 °C. The CMC value was determined from Figure 1C,D.

concentrations are less accurate because this dye may form nonemissive aggregates in water, causing a decrease of fluorescence intensity and an increase of experimental uncertainty.[43,44] However, for polymer concentrations higher than 0.01 g L^{-1}, an increase of r_{ss} is observed for both probes. Since this concentration is almost 10 times lower than the CMC (0.074 g L^{-1}; average value), these results suggest the presence of premicellar aggregates. Indeed, when the polymer concentration increases above a certain value, premicellar aggregates of a few polymer chains are formed, increasing the fluorescence anisotropy due to the loss of rotation mobility of the dye located in those aggregates.

Although the formation of premicellar aggregates could be induced by the presence of the probe in the aqueous medium, the coincident increase of r_{ss} at the same block copolymer concentration for both C153 and ORB probes suggests a spontaneous aggregation process. To deeply understand the formation of the premicellar aggregates and the dynamics of the probes in both the premicellar aggregates and the micelle core, time-resolved fluorescence anisotropy measurements were performed.

Time-Resolved Fluorescence Anisotropy. Organic fluorophores dissolved in pure solvents undergo free Brownian rotational motion and, consequently, the anisotropy decays to zero (total depolarization).[45] The anisotropy decay of anisotropic rotors is complex (a sum of 5 exponentials is predicted for the most complex case) since the three principal rotational axes are not equivalent and the absorption and emission transition moments cannot be directed along one of the principal axes.[45−47] However, often only one average correlation time is observed because the anisotropy decay curve has a very small dynamic range not allowing the discrimination between the diffusion rotational correlation times that usually do not differ significantly. On the other hand, in a spherical micelle, a monoexponential anisotropy decay is seldom observed. Several models have been proposed to describe the dynamics of a fluorescent probe in a micelle.[15] Generally, two contributions are considered: (i) micelle rotation in aqueous solution (*slow reorientation time*) and (ii) molecular dynamics of the probe in the micelle (*fast reorientation time*).[10−12,16,17] The dynamics of the probe in the micelle depends namely on the location of the probe in the micelle and on its molecular structure. Usually, the probe can display two kinds of motion: a slow diffusion (lateral or rotational) and a fast wobbling motion in a cone around an imaginary axis. If these motions are uncorrelated, the resulting anisotropy decay is given by

$$r(t) = r_M(t) \times r_L(t) \times r_W(t) \quad (2)$$

where $r_M(t)$, $r_L(t)$, and $r_W(t)$ are respectively the anisotropy decay corresponding to the rotation of the micelle, the lateral/rotational diffusion of the probe, and its wobbling motion in a cone. The anisotropy decays for the rotation of the micelle as a whole and the lateral/rotational motion of the probe are usually expressed as single exponentials,

$$r_M(t) = r_0 \exp\left(-\frac{t}{\theta_M}\right) \quad (3a)$$

$$r_L(t) = r_0 \exp\left(-\frac{t}{\theta_{agg}}\right) \quad (3b)$$

where θ_M and θ_{agg} are the correlation times for the rotation of the micelle as a whole and the lateral/rotational diffusion of the probe and r_0 is the fundamental anisotropy that varies with the orientation of the transition dipole moments for the absorption and the emission, presenting a maximum value of 0.4 when the transition dipole moments are collinear.

The *wobbling-in-a-cone* model considers that the probe undergoes a nonisotropic motion, wobbling around an axis within a cone characterized by a certain semiangle.[48] The anisotropy decay component of this motion is given by

$$r_W(t) = r_0[(1 - S^2)\exp(-t/\theta_W) + S^2] \quad (4)$$

where θ_W is the correlation time for the wobbling-in-a-cone motion and S is a generalized order parameter reflecting the degree of orientational constraint imposed by the surroundings. If the motion is isotropic, $S = 0$, and if it is completely restricted, $|S| = 1$.[48,49]

Then, the global anisotropy, considering all the contributions, is given by

$$r(t) = r_0\left[S^2 \exp\left(-\frac{t}{\theta_1}\right) + (1 - S^2)\exp\left(-\frac{t}{\theta_2}\right)\right] \quad (5)$$

where θ_1 and θ_2 are the global correlation times, related to the model parameters by

$$\frac{1}{\theta_1} = \frac{1}{\theta_{agg}} + \frac{1}{\theta_M} \quad (6a)$$

$$\frac{1}{\theta_2} = \frac{1}{\theta_W} + \frac{1}{\theta_1} = \frac{1}{\theta_W} + \frac{1}{\theta_{agg}} + \frac{1}{\theta_M} \quad (6b)$$

For a spherical particle (such as a micelle), θ_M can be estimated using the Debye−Stokes−Einstein relation:[50]

$$\theta_M = \frac{\eta V_h f}{k_B T} = \frac{\eta 4\pi R_h^3 f}{3k_B T} \quad (7)$$

where η is the solvent viscosity, V_h is the hydrodynamic volume, f is a frictional coefficient ($f = 1$ in the stick boundary limit), k_B is the Boltzmann constant, T (in K) is the absolute temperature, and R_h is the hydrodynamic radius. For instance, in the stick boundary limit, a correlation time of 6.26 μs was obtained for the $PDcA_{11}$-*block*-$PDEA_{295}$ micelles in water at 20 °C (hydrodynamic radius, $R_h = 18.2$ nm).[40] Such rotational motion of the micelle is very slow and cannot be measured with the usual fluorescent probes that present intrinsic lifetimes of the order of some nanoseconds. This allowed us to simplify eqs 6a and 6b to

$$\frac{1}{\theta_1} = \frac{1}{\theta_{agg}} \quad (8a)$$

$$\frac{1}{\theta_2} = \frac{1}{\theta_W} + \frac{1}{\theta_1} = \frac{1}{\theta_W} + \frac{1}{\theta_{agg}} \quad (8b)$$

The global anisotropy decay is described by a sum of two exponentials (eq 5) with fast ($\theta_{fast} = \theta_2$) and slow ($\theta_{slow} = \theta_1$) correlation times. If the rotational/lateral motion of the probe is strongly restricted, $\theta_{slow} = \theta_{agg} \sim \infty$, and the anisotropy decays to a constant value at long times, r_∞,[48] the anisotropy decay is then given by

$$r(t) = r_0\left[S^2 + (1 - S^2)\exp\left(-\frac{t}{\theta_2}\right)\right] \quad (9)$$

If the probe is partitioned between several environments, the anisotropy is described by the associated anisotropy model, in which the anisotropy decay is a fluorescence intensity weighted average of the contribution from the probe in each environment:[51]

$$r(t) = \sum_i f_i(t) \times r_i(t) \quad (10)$$

where the fractional time dependent intensities, $f_i(t)$ are determined by the fluorescence decays in each environment. If the probe displays a single exponential decay with lifetime (τ_m) and a single correlation time (θ_m) in each mth environment, the global anisotropy is given by

$$r(t) = \frac{\sum_m \alpha_m \exp(-t/\tau_m)\beta_m \exp(-t/\theta_m)}{\sum_m \alpha_m \exp(-t/\tau_m)} \quad (11)$$

with the decays normalized to 1 at time zero ($\Sigma_m \alpha_m = 1$) and the sum of the pre-exponential factor of the individual anisotropy decay components equal to the limiting anisotropy ($\Sigma_m \beta_m = r_0$).

Anisotropy Decays for ORB. Figure 3 shows the fluorescence (A) and anisotropy (B) decays of ORB in aqueous solutions of $PDcA_{11}$-*block*-$PDEA_{295}$ at concentrations ranging from 0 to 0.23 g L^{-1}.

The fluorescence decays were well fitted with a sum of 2 or 3 exponentials (Table 1), $I(t) = \Sigma_i \alpha_i \exp(-t/\tau_i)$, as judged by the reduced χ^2 (close to 1) and the random distribution of weighted residuals around zero.

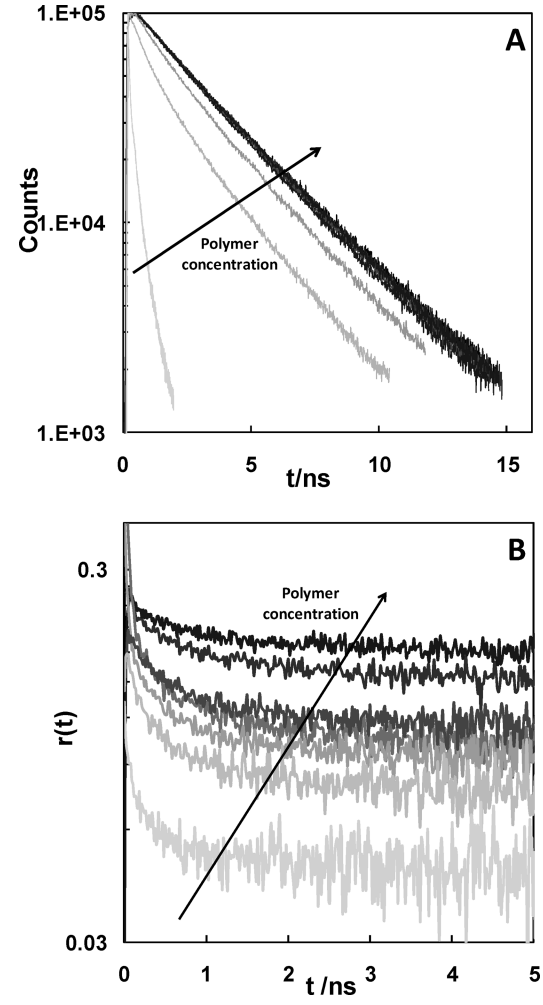

Figure 3. Fluorescence emission (A) and anisotropy (B) decays of ORB (0.5 μM) in aqueous solutions of $PDcA_{11}$-*block*-$PDEA_{295}$ at several block copolymer concentrations (0−0.23 g L^{-1}). $\lambda_{exc} = 570$ nm, $\lambda_{em} = 610$ nm; $T = 20$ °C.

Similar complex decays were found for ORB in Triton X-100 micelles, AOT reverse micelles, and in pure organic solvents like hexane and dodecane.[14] Since this probe is highly hydrophobic, it is very probable that it locates in hydrophobic regions like the premicellar aggregates and the micelle core. For copolymer concentrations above the CMC, the decay can be fitted with a sum of two exponentials with a short lifetime component of $\tau_1 = 1.8 \pm 0.1$ ns and a dominant component of $\tau_2 = 3.8 \pm 0.1$ ns. For lower copolymer concentrations and in pure water, the lifetimes are smaller due to both the self-quenching and the quenching by water.[52]

The anisotropy of ORB decays to a nonzero constant value at long times ($r_\infty \neq 0$) that increases for higher $PDcA_{11}$-*block*-$PDEA_{295}$ block copolymer concentrations (Figure 3B). This differs from the behavior in Triton X-100,[14] SDS, CTAB, and Thesit micelles[53] and AOT reversed micelles,[19] for which the anisotropy decay curve can be well fitted by a sum of two exponentials. This clearly indicates that a fraction of the ORB molecules located in the micelle core do not move. The core is probably composed of semicrystalline regions formed by the decyl hydrocarbon chains that can incorporate the octadecyl tail of the ORB dye, hindering its global rotational motion, while other fraction of ORB molecules located in amorphous regions

TABLE 1: Fluorescence and Anisotropy Decay Parameters for ORB (0.5 μM) in Aqueous Solutions of $PDcA_{11}$-*block*-$PDEA_{295}$ at Increasing Block Copolymer Concentrations[a]

[polymer]/g L^{-1}	α_i	τ_i/ns	$\langle\tau\rangle$/ns	β_1	θ_1/ns	β_2	θ_2/ps	r_∞	r_0
0	0.20	0.85	0.36						
	0.80	0.24							
1.4×10^{-2}	0.37	3.15	1.67	0.07 ± 0.01	0.17 ± 0.02	0.21 ± 0.01	9 ± 1	0.05 ± 0.01	0.33 ± 0.02
	0.32	1.26							
	0.31	0.37							
4.9×10^{-2}	0.65	3.37	2.62	0.06 ± 0.01	0.24 ± 0.04	0.25 ± 0.01	15 ± 2	0.05 ± 0.01	0.35 ± 0.03
	0.35	1.24							
5.4×10^{-2}	0.68	3.63	3.04	0.09 ± 0.01	0.37 ± 0.02	0.16 ± 0.01	15 ± 2	0.08 ± 0.01	0.32 ± 0.03
	0.32	1.79							
6.6×10^{-2}	0.76	3.67	3.19	0.07 ± 0.01	0.55 ± 0.08	0.19 ± 0.01	37 ± 6	0.08 ± 0.01	0.34 ± 0.04
	0.24	1.67							
8.3×10^{-2}	0.66	3.75	3.11	0.06 ± 0.01	0.64 ± 0.02	0.20 ± 0.02	59 ± 15	0.07 ± 0.02	0.33 ± 0.02
	0.34	1.89							
1.0×10^{-1}	0.68	3.79	3.19	0.06 ± 0.01	1.04 ± 0.25	0.16 ± 0.02	60 ± 18	0.10 ± 0.01	0.32 ± 0.01
	0.32	1.91							
1.6×10^{-1}	0.69	3.84	3.19	0.05 ± 0.01	1.09 ± 0.22	0.09 ± 0.02	62 ± 27	0.18 ± 0.01	0.32 ± 0.02
	0.31	1.78							
2.3×10^{-1}	0.69	3.77	3.15	0.07 ± 0.01	1.02 ± 0.16	0.10 ± 0.01	50 ± 19	0.15 ± 0.01	0.32 ± 0.02
	0.31	1.78							

[a] CMC = 7.4×10^{-2} g L^{-1}.

of the core can still rotate. If we assume that the probe has a similar wobbling motion in both domains (which sounds reasonable due to its long hydrophobic tail), then the anisotropy decay must contain the contribution from both these locations. So, considering that the fraction of ORB molecules in the semicrystalline region is γ, its rotational motion is hindered ($\theta_{agg} \sim \infty$) and the fluorescence decay is identical in both domains, the global anisotropy decay is given by the sum of the contributions of the ORB molecules in each region. Consequently, taking into account eqs 8a and 8b, the global anisotropy decay can be expressed as

$$r(t) = r_0\left\{(1-\gamma)\left[S^2\exp\left(-\frac{t}{\theta_1}\right) + (1-S^2)\exp\left(-\frac{t}{\theta_2}\right)\right] + \gamma\left[S^2 + (1-S^2)\exp\left(-\frac{t}{\theta_2}\right)\right]\right\}$$
$$= r_0\left[(1-\gamma)S^2\exp\left(-\frac{t}{\theta_1}\right) + (1-S^2)\exp\left(-\frac{t}{\theta_2}\right) + \gamma S^2\right] \quad (12)$$

which can be more simply written as a sum of two exponentials plus a constant,

$$r(t) = \beta_1\exp(-t/\theta_1) + \beta_2\exp(-t/\theta_2) + r_\infty \quad (13)$$

with $\beta_1 + \beta_2 + r_\infty = r_0$, the limiting anisotropy in the absence of rotation.

Table 1 summarizes the recovered parameters from the fitting of the fluorescence and anisotropy decays of ORB (0.5 μM) in aqueous solutions of $PDcA_{11}$-*block*-$PDEA_{295}$.

The variation of the lifetimes (A) and correlation times (B) of the ORB probe with $PDcA_{11}$-*block*-$PDEA_{295}$ concentration in aqueous solutions is shown in Figure 4. The lifetimes (τ_i; $i = 1-3$) and the corresponding average lifetime ($\langle\tau\rangle = \Sigma_i\alpha_i\tau_i/\Sigma_i\alpha_i$) increase with polymer concentration to reach almost constant values for polymer concentration above the CMC. Figure 4A shows that the lifetimes do not increase steeply *at* the CMC but instead begin to increase at polymer concentrations *below but close* to the CMC, again suggesting the formation of premicellar aggregates. A similar behavior can be observed in Figure 4B for the slow (θ_1) and fast (θ_2) correlation times.

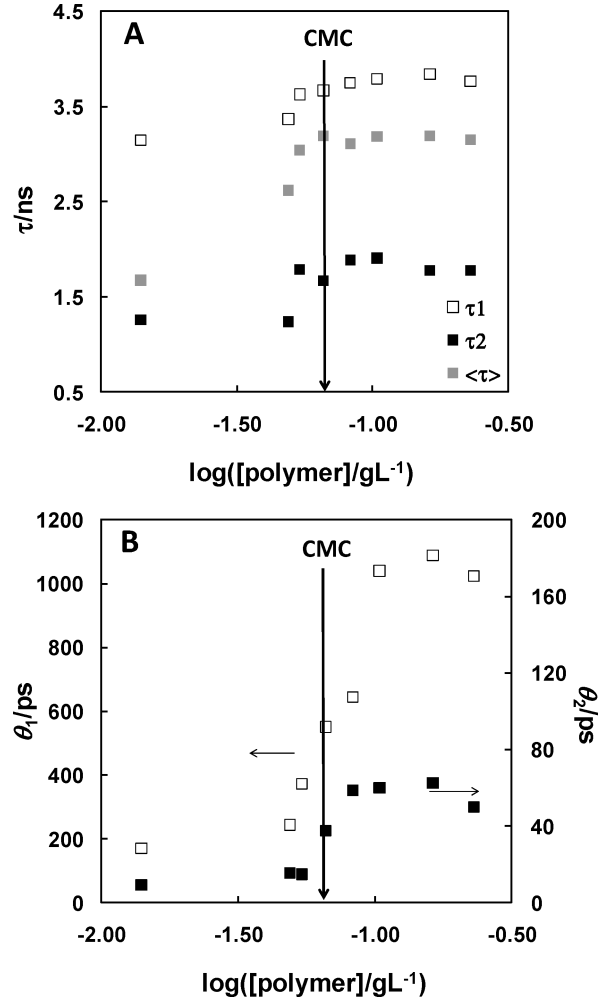

Figure 4. Plots of lifetimes (A) and correlation times (B) of fluorescence and anisotropy decays of ORB (0.5 μM) as a function of $PDcA_{11}$-*block*-$PDEA_{295}$ concentration (in logarithmic scale). The CMC value was obtained from Figure 1C,D.

DelaCruz and Blanchard have previously observed that ORB exhibits monoexponential anisotropy decay in water with a correlation time of $\theta_{ORB,water} = 145 \pm 21$ ps.[53] The correlation

time observed for the most dilute block copolymer solution (1.4×10^{-2} g L^{-1}) is $\theta_1 = 170$ ps, which suggests that at this polymer concentration the environment of the ORB molecule is similar to bulk water. Besides, we observe a fast correlation time of 9 ps, difficult to detect in water, which was attributed to the local motion of the ORB molecule around the C_{10} alkyl chain, similarly to the anisotropy behavior of rhodamine X labeled oligonucleotides.[54,55] The correlation time corresponding to the rotational motion of ORB in the micelle core $\theta_1 \sim \theta_{agg}$ increases within the premicellar region (4.9×10^{-2} to 1.0×10^{-1} g L^{-1}) to attain an almost constant value (1.0−1.1 ns) for concentrations greater than 1.0×10^{-1} g L^{-1}. This suggests that ORB molecules will interact with sparsely formed premicellar aggregates below the CMC and migrate to the micelle core for concentrations above the CMC, causing a slower motion of the dye and a subsequent increase of the correlation time. A similar trend was obtained for the θ_2 values, which increase in the premicellar region from 15 to 60 ps to remain almost constant (60 ps) for concentrations above the CMC. However, the variation of the shorter correlation time, θ_2, is much less significant (ca. 35 ps), which supports the hypothesis of a local conformational motion.

The r_∞ values also increase with block copolymer concentration, showing that a larger fraction of immobile molecules is present. The fraction of immobile (i.e., located in the semicrystalline regions) ORB molecules, γ, and the order parameter S could be determined from the values of β_1, β_2, and r_∞. Unfortunately, the uncertainty in the fitted values did not allow a precise determination of these parameters. Nevertheless, a tendency of increase in both S^2 and γ values with polymer concentration was observed. The calculated values vary in the interval of $0.3 < S^2 < 0.7$ and $0.4 < \gamma < 0.8$.

The limiting anisotropy of ORB in aqueous solutions of $PDcA_{11}$-*block*-$PDEA_{295}$, $r_0 = 0.34 \pm 0.02$, is slightly lower than the previously determined value for this dye ($r_0 = 0.375$),[56] indicating that some instrumental artifacts and other fast depolarization process (such as scattering depolarization of emission and/or excitation) may be present.

Anisotropy Decays for C153. The anisotropy decays of C153 dye in aqueous solutions of $PDcA_{11}$-*block*-$PDEA_{295}$ show a completely different profile than the corresponding curves for the ORB probe (Figure 5). The C153 anisotropy decays are typical of an associated system, in which the dye is partitioned between two (or more) environments presenting different fluorescence decays in each environment. The fluorescence decays can be well fitted with a sum of two exponentials (Table 2). In pure water, the decay has a dominant component (∼97%) of 1.75 ns and a residual (∼3%) component of 3.88 ns. A single exponential decay is expected from this dye because the interconversion between the intramolecular (ICT) excited state and the twisted intramolecular CT state (TICT) is hindered due to the structural rigidity of coumarin C153. Indeed, a single exponential decay was observed in several solvents with lifetimes between 4.0 and 6.0 ns.[57] The residual component 3.88 ns is probably due to the aggregation of this dye since its solubility in water is very low, 2×10^{-6} M.[58] The major decay component of 1.75 ns is attributed to the free dye in water. The lifetime is lower than the usual values found for this dye in other solvents due to the quenching by water.[59] For all polymer solutions, the decays were fitted with two lifetime components of 1.8 ± 0.1 and 6.3 ± 0.2 ns. The component of 1.8 ns is associated with the C153 molecules in the water phase, while the component of 6.3 ns is attributed to the C153 molecules located in the premicellar aggregates or the micelle core. The

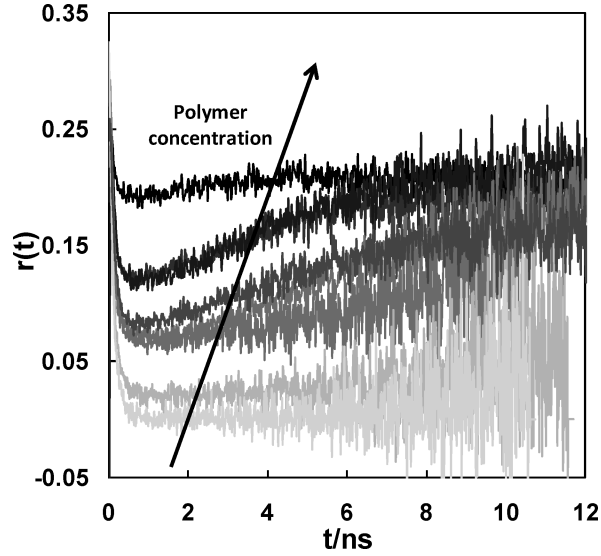

Figure 5. Anisotropy decays of C153 (0.45 μM) in aqueous solutions of $PDcA_{11}$-*block*-$PDEA_{295}$ at several block copolymer concentrations (0−0.23 g L^{-1}). $\lambda_{exc} = 420$ nm, $\lambda_{em} = 530$ nm; $T = 20$ °C.

pre-exponential factor of each decay component is a measure of the fraction of C153 molecules in each environment. The fraction of molecules in the premicellar aggregates/micelle core increases with the polymer concentration, from about 12% (4.9×10^{-2} g L^{-1}) to 57% at the highest concentration (2.3×10^{-1} g L^{-1}).

As observed in Figure 5, the anisotropy decay decreases from the limiting anisotropy value (∼0.4), then passes through a minimum and increases afterward to reach a plateau at long times. This unusual anisotropy behavior is rarely observed and results from the fact that C153 is partitioned between two different environments, the aqueous medium and the premicellar aggregates or micelle core, and its fluorescence decay depends on the polarity of the environment.[51] In the aqueous medium, C153 has a free isotropic rotation and a rapid deactivation of excited state; in the premicellar aggregates or micelle core, the probe presents a larger rotational correlation time, θ_{agg}, and larger fluorescence lifetimes. Consequently, the anisotropy decays of C153 are described by the associated anisotropy model (eq 9) with two components:[51]

$$r(t) = f_{aq}(t) \times r_{aq}(t) + f_{agg}(t) \times r_{agg}(t) \tag{14}$$

one corresponding to C153 in aqueous environment,

$$r_{aq}(t) = r_0 \exp(-t/\theta_{aq}) \tag{15a}$$

and the other corresponding to C153 within the micelle and/or premicellar aggregates

$$r_{agg}(t) = r_0[(1 - \delta) \exp(-t/\theta_{agg}) + \delta] = (r_0 - r_\infty) \exp(-t/\theta_{agg}) + r_\infty \tag{15b}$$

where δ is the fraction of C153 molecules located in the semicrystalline regions, where the probe motion is hindered, $\theta_{agg} \sim \infty$. In this case, the wobbling-in-a-cone motion was not considered because C153 does not have the hydrophobic tail around which the fluorophore can move.

TABLE 2: Fluorescence Emission and Anisotropy Decay Parameters for C153 (~0.45 μM) in Aqueous Solutions of $PDcA_{11}$-*block*-$PDEA_{295}$ at Increasing Block Copolymer Concentrations[a]

[polymer]/g L^{-1}	α_i	τ_i/ns	$\langle\tau\rangle$/ns	x_{aq}	θ_{aq}/ps	x_{agg}	θ_{agg}/ps	r_∞	r_0	$\delta = r_\infty/r_0$
0	0.03	3.88	1.81	1	85				0.31	
	0.97	1.75								
4.9×10^{-2}	0.12	6.23	2.42	0.70 ±	85	0.30 ±	425 ± 61	0.14 ± 0.002	0.40 ± 0.02	0.35
	0.88	1.90		0.01		0.01				
6.6×10^{-2}	0.17	6.07	2.61	0.66 ±	85	0.34 ±	390 ± 58	0.16 ± 0.001	0.40 ± 0.01	0.40
	0.83	1.89		0.01		0.01				
8.3×10^{-2}	0.19	6.26	2.42	0.64 ±	85	0.36 ±	400 ± 74	0.16 ± 0.002	0.40 ± 0.01	0.40
	0.81	1.91		0.02		0.02				
1.0×10^{-1}	0.23	6.22	2.86	0.58 ±	85	0.42 ±	420 ± 150	0.22 ± 0.002	0.40 ± 0.03	0.55
	0.77	1.88		0.02		0.02				
1.6×10^{-1}	0.47	6.41	3.99	0.53 ±	85	0.47 ±	400 ± 95	0.20 ± 0.002	0.38 ± 0.02	0.53
	0.53	1.80		0.02		0.02				
2.3×10^{-1}	0.57	6.46	4.45	0.23 ±	85	0.77 ±	390 ± 87	0.21 ± 0.001	0.35 ± 0.01	0.63
	0.43	1.79		0.03		0.03				

[a] θ_{aq} was fixed to 85 ps. CMC = 7.4×10^{-2} g L^{-1}.

The fractional time-dependent intensities for C153 in each environment are given by

$$f_{aq}(t) = \frac{\alpha_{aq,1}\exp(-t/\tau_{aq,1}) + \alpha_{aq,2}\exp(-t/\tau_{aq,2})}{\alpha_{aq,1}\exp(-t/\tau_{aq,1}) + \alpha_{aq,2}\exp(-t/\tau_{aq,2}) + \alpha_{agg}\exp(-t/\tau_{agg})} \quad (16a)$$

$$f_{agg}(t) = \frac{\alpha_{agg}\exp(-t/\tau_{ag})}{\alpha_{aq,1}\exp(-t/\tau_{aq,1}) + \alpha_{aq,2}\exp(-t/\tau_{aq,2}) + \alpha_{agg}\exp(-t/\tau_{agg})} \quad (16b)$$

where $\alpha_{aq,1}$, $\alpha_{aq,2}$, $\tau_{aq,1}$, $\tau_{aq,2}$, and α_{agg}, τ_{agg} are the corresponding amplitudes and lifetimes for the two populations considering that the fluorescence decay of C153 is biexponential in water and monoexponential within the premicellar aggregates or micelles. If we assume that the molar absorption coefficient and the radiative rate constant are the same for the two populations, it is possible to calculate from the anisotropy fittings (eq 14), the molar fractions (x_{aq} and x_{agg}) of each dye population. The anisotropy decay of C153 in water was found to be monoexponential with a correlation time of $\theta_{aq} = 85$ ps. Hence, the anisotropy decays were fitted using eq 14 fixing $\theta_{aq} = 85$ ps, and the fluorescence decays in water ($\alpha'_{aq,1} = 0.03$, $\tau_{aq,1} = 3.88$ ns, $\alpha'_{aq,2} = 0.97$, $\tau_{aq,2} = 1.75$ ns) and in the aggregates ($\alpha'_{agg} = 1$ and τ_{agg} equal to the longer lifetime of the fluorescence decay for each copolymer solution). Figure 6 shows a typical experimental anisotropy decay curve fitted with eq 14. The fitting to the experimental data is very reasonable, as judged by the residuals that are randomly distributed around zero. The small deviation at short times is probably due to a residual component of light scattering and the uncertainty introduced in the calculation of the anisotropy decay from the polarized fluorescence decay components. Table 2 summarizes the fitted parameters: x_{agg} (and $x_{aq} = 1 - x_{agg}$), r_∞, r_0, and θ_{agg}.

The θ_{agg} is practically constant for all polymer concentrations, not providing additional information about the presence of premicellar aggregates. Nevertheless, the fraction of C153 in the premicellar aggregates ($x_{agg} \sim 0.34$) is always lower than in the micelles ($x_{agg} \sim 0.45$). The anisotropy values at long times (r_∞) are also lower in the premicellar aggregates ($r_\infty \sim 0.16$) than in the micelle cores ($r_\infty \sim 0.22$), due to the increase of the fraction of probe located in the semicrystalline domains (δ) from about 0.40 in the premicellar aggregates to about 0.55 in the micelle core, which is in agreement with the γ values calculated with the ORB dye.

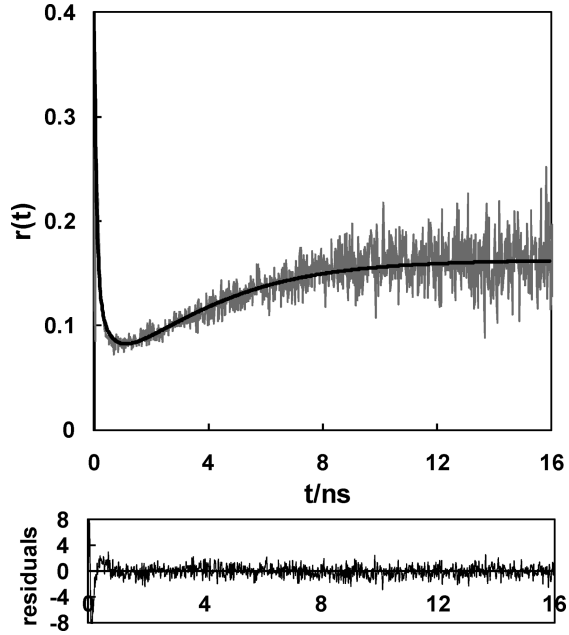

Figure 6. Fluorescence anisotropy decay and fitting curve using eq 14 of C153 (0.45 μM) in aqueous solution of $PDcA_{11}$-*block*-$PDEA_{295}$ at 8.3×10^{-2} g L^{-1}. $\lambda_{exc} = 420$ nm, $\lambda_{em} = 530$ nm; $T = 20$ °C.

Comparison between Probes and Estimation of the Viscosity of Micelle Core. As shown above, C153 is always partitioned between two environments. However, the fraction of C153 within the preaggregates/micelles increases when the block copolymer concentration increases. Besides, the value of the rotational correlation time is almost constant ($\theta_{agg} \approx 400$ ps), regardless of the type of aggregate in which the probe is located (premicellar aggregates or micelle core). The corresponding rotational correlation time for ORB is more sensitive to the kind of aggregates, increasing with polymer concentration in the premicellar region to attain a constant value of $\theta_{agg} \sim 1.0$ ns in the micelle core. The differences in these values should be correlated with the difference in the hydrodynamic volumes of the two probes (717 $Å^3$ for ORB[53] and 246 $Å^3$ for C153[20]). It is expected from the Stokes−Einstein relation (eq 7) that the ratio between the correlation times of ORB and C153 within

the micelle is directly proportional to the ratio between their hydrodynamic volumes. In fact, $\theta_{agg}^{ORB}/\theta_{agg}^{C153} = 2.5$, which is close to the ratio of hydrodynamic volumes, $V_h^{ORB}/V_h^{C153} = 2.9$; the differences can be attributed to different friction coefficients (f) of the probes.

Using the Stokes−Einstein relation at the stick boundary limit, it was also possible to estimate from eq 7 the effective viscosity of the amorphous region of the micelle core, $\eta_{PDcA\ core} = 6.3 \pm 0.5$ cP. This value is lower than the values found for SDS ($\eta =$ 193 cP[60]) and CTAB ($\eta = 19-30$ cP[61] or 151 cP[60]) micelles, reflecting the larger free volume in the amorphous polymer regions when compared to the core of alkyl chains of the low molecular weight surfactants. It is worth noting that in the case of the low molecular weight surfactants, the probes can be located near the interface of the micelle and display a lateral motion that cannot be compared to the rotational motion of the probe in the copolymer micelles whose radii is around 4 times larger ($R_h \sim 4$ nm) than the typical radii of low molecular weight surfactant ($R_h \sim 1$ nm). In addition, ORB presents a faster rotational motion than expected on the basis of its hydrodynamic volume and considering the stick boundary limit ($f = 1$ in eq 7), which was explained by a more "slip-like" behavior of this probe.[53]

Conclusions

The steady-state fluorescence anisotropy of coumarin 153 (C153) and octadecylrhodamine B (ORB) show the presence of premicellar aggregates of $PDcA_{11}$-*block*-$PDEA_{295}$ block copolymers in water below the CMC (1.8 ± 0.1 μM), which was determined from both the fluorescence intensity and the solvatochromic shifts of C153.

The anisotropy decay curves of C153 and ORB in both the premicellar region and above the CMC are different. This is explained by a different partition of the probes between the water phase and the premicellar aggregates/micelle core. While the very hydrophobic ORB probe is located in the premicellar aggregates/micelle core, C153 is partitioned between the water phase and the hydrophobic domains of the polymer aggregates. The ORB probe undergoes a fast wobbling-in-a-cone motion not observed for the C153 dye, which was attributed to the long alkyl chain of this molecule.

Moreover, this study shows that the aggregates are composed of both semicrystalline regions where probes are immobilized and amorphous regions where the probes can more or less freely rotate.

Finally, the ratio of correlation times for ORB ($\theta_{agg}^{ORB} \sim 1.0$ ns) and C153 ($\theta_{agg}^{C153} \sim 400$ ps) probes of 2.5 is in agreement with the corresponding ratio of their hydrodynamic volumes, $V_h^{ORB}/V_h^{C153} = 2.9$. The viscosity of the amorphous region of the core of 6.3 cP denotes a fluid region probably due to the large free-volume accessible for the free rotation of the probes.

Acknowledgment. We thank Dr. Telmo Prazeres for the synthesis of the block copolymer sample and Prof. Mário N. Berberan-Santos for the fruitful discussions and help with the analysis software. Mariana Beija acknowledges Fundação para a Ciência e Tecnologia for her Ph.D. grant (SFRH/BD/18562/2004).

References and Notes

(1) *Amphiphilic block copolymers - self-assembly and applications*; Alexandridis, P., Lindman, B., Eds.; Elsevier: Amsterdam, 2000.
(2) Maibaum, L.; Dinner, A. R.; Chandler, D. *J. Phys. Chem. B* **2004**, *108*, 6778.
(3) Sabaté, R.; Gallardo, M.; Estelrich, J. *Electrophoresis* **2000**, *21*, 481.
(4) Zettl, H.; Portnoy, Y.; Gottlieb, M.; Krausch, G. *J. Phys. Chem. B* **2005**, *109*, 13397.
(5) Cui, X.; Mao, S.; Liu, M.; Yuan, H.; Du, Y. *Langmuir* **2008**, *24*, 10771.
(6) Barnadas-Rodríguez, R.; Estelrich, J. *J. Phys. Chem. B* **2009**, *113*, 1972.
(7) Hadgiivanova, R.; Diamant, H. *J. Phys. Chem. B* **2007**, *111*, 8854.
(8) Hadgiivanova, R.; Diamant, H. *J. Chem. Phys.* **2009**, *130*, 114901.
(9) Mackie, A. D.; Panagiotopoulos, A. Z.; Szleifer, I. *Langmuir* **1997**, *13*, 5022.
(10) Maiti, N. C.; Krishna, M. M. G.; Britto, P. J.; Periasamy, N. *J. Phys. Chem. B* **1997**, *101*, 11051.
(11) Kelepouris, L.; Blanchard, G. J. *J. Phys. Chem. B* **2002**, *106*, 6600.
(12) Kelepouris, L.; Blanchard, G. J. *J. Phys. Chem. B* **2003**, *107*, 1079.
(13) Dutt, G. B. *Langmuir* **2005**, *21*, 10391.
(14) Visser, A. J. W. G.; Vos, K.; Van Hoek, A.; Santema, J. S. *J. Phys. Chem.* **1988**, *92*, 759.
(15) Periasamy, N. *J. Fluoresc.* **2001**, *11*, 161.
(16) Dutt, G. B. *J. Phys. Chem. B* **2002**, *106*, 7398.
(17) Dutt, G. B. *J. Phys. Chem. B* **2003**, *107*, 3131.
(18) Dutt, G. B. *J. Phys. Chem. B* **2003**, *107*, 10546.
(19) Dutt, G. B. *J. Phys. Chem. B* **2008**, *112*, 7220.
(20) Grant, C. D.; Steege, K. E.; Bunagan, M. R.; Castner, E. W. *J. Phys. Chem. B* **2005**, *109*, 22273.
(21) Dutt, G. B. *J. Phys. Chem. B* **2005**, *109*, 4923.
(22) Horng, M. L.; Gardecki, J. A.; Papazyan, A.; Maroncelli, M. *J. Phys. Chem.* **1995**, *99*, 17311.
(23) Argaman, R.; Huppert, D. *J. Phys. Chem. B* **2000**, *104*, 1338.
(24) Bart, E.; Meltsin, A.; Huppert, D. *J. Phys. Chem.* **1994**, *98*, 3295.
(25) Chakrabarty, D.; Chakraborty, A.; Seth, D.; Sarkar, N. *J. Phys. Chem. A* **2005**, *109*, 1764.
(26) Chakraborty, A.; Seth, D.; Chakrabarty, D.; Setua, P.; Sarkar, N. *J. Phys. Chem. A* **2005**, *109*, 11110.
(27) Kim, T. G.; Topp, M. R. *J. Phys. Chem. A* **2004**, *108*, 7653.
(28) Krolicki, R.; Jarzeba, W.; Mostafavi, M.; Lampre, I. *J. Phys. Chem. A* **2002**, *106*, 1708.
(29) Molotsky, T.; Huppert, D. *J. Phys. Chem. A* **2002**, *106*, 8525.
(30) Molotsky, T.; Huppert, D. *J. Phys. Chem. A* **2003**, *107*, 2769.
(31) Molotsky, T.; Huppert, D. *J. Phys. Chem. A* **2003**, *107*, 8449.
(32) Tamoto, Y.; Segawa, H.; Shirota, H. *Langmuir* **2005**, *21*, 3757.
(33) Frauchiger, L.; Shirota, H.; Uhrich, K. E.; Castner, E. W. *J. Phys. Chem. B* **2002**, *106*, 7463.
(34) Grant, C. D.; DeRitter, M. R.; Steege, K. E.; Fadeeva, T. A.; Castner, E. W. *Langmuir* **2005**, *21*, 1745.
(35) Kumbhakar, M.; Goel, T.; Nath, S.; Mukherjee, T.; Pal, H. *J. Phys. Chem. B* **2006**, *110*, 25646.
(36) Ediger, M. D. D., R. P.; Fayer, M. D. *J. Chem. Phys.* **1984**, *80*, 1246.
(37) Berberan-Santos, M. N.; Prieto, M. *J. Chem. Soc., Faraday Trans. II* **1987**, *83*, 1391.
(38) Prazeres, T. J. V.; Beija, M.; Farinha, J. P. S.; Charreyre, M. T.; Martinho, J. M. G. *Polymer* **2010**, *51*, 355.
(39) Farinha, J. P. S.; Relógio, P.; Charreyre, M. T.; Prazeres, T. J. V.; Martinho, J. M. G. *Macromolecules* **2007**, *40*, 4680.
(40) Marcelo, G.; Prazeres, T. J. V.; Charreyre, M. T.; Martinho, J. M. G.; Farinha, J. P. S. *Macromolecules* **2010**, *43*, 501.
(41) Castro, E.; Barbosa, S.; Juárez, J.; Taboada, P.; Katime, I. A.; Mosquera, V. *J. Phys. Chem. B* **2008**, *112*, 5296.
(42) Castro, E.; Taboada, P.; Mosquera, V. *J. Phys. Chem. B* **2006**, *110*, 13113.
(43) Mukerjee, P. *J. Phys. Chem.* **1965**, *69*, 2821.
(44) Humpolickova, J.; Prochazka, K.; Hof, M.; Tuzar, Z.; Spirkova, M. *Langmuir* **2003**, *19*, 4111.
(45) Valeur, B. *Molecular Fluorescence - Principles and Applications*; Wiley VCH: Weinheim, 2002.
(46) Chuang, T. J.; Eisenthal, K. B. *J. Chem. Phys.* **1972**, *57*, 5094.
(47) Belford, R. L.; Weber, G. *Proc. Natl. Acad. Sci. U.S.A.* **1972**, *69*, 1392.
(48) Lipari, G.; Szabo, A. *Biophys. J.* **1980**, *30*, 489.
(49) Quitevis, E. L.; Marcus, A. H.; Fayer, M. D. *J. Phys. Chem.* **1993**, *97*, 5762.
(50) Debye, P. *Polar Molecules*; Dover: New York, 1929.
(51) Lakowicz, J. R. *Principles of Fluorescence Spectroscopy*, 3rd ed.; Springer: New York, 2006.
(52) Magde, D.; Rojas, G. E.; Seybold, P. G. *Photochem. Photobiol.* **1999**, *70*, 737.
(53) DelaCruz, J. L.; Blanchard, G. J. *J. Phys. Chem. B* **2003**, *107*, 7102.
(54) Prazeres, T. J. V.; Santos, A. M.; Martinho, J. M. G. *Langmuir* **2004**, *20*, 6834.

(55) Prazeres, T. J. V.; Fedorov, A.; Martinho, J. M. G. *J. Phys. Chem. B* **2004**, *108*, 9032.
(56) Johansson, L. B.-A. *J. Chem. Soc., Faraday Trans.* **1990**, *86*, 2103.
(57) Lewis, J. E.; Maroncelli, M. *Chem. Phys. Lett.* **1998**, *282*, 197.
(58) Jones, G.; Jackson, W. R.; Choi, C.; Bergmark, W. R. *J. Phys. Chem.* **1985**, *89*, 294.
(59) Jones II, G.; Rahman, M. A. *J. Phys. Chem.* **1994**, *98*, 13028.
(60) Pownall, H. J.; Smith, L. C. *J. Am. Chem. Soc.* **1973**, *95*, 3136.
(61) Shinitzkey, M.; Dianox, A. C.; Gitter, C.; Webber, G. *Biochemistry* **1971**, *10*, 2106.

JP101613Y